On the robustness of estimates of mechanical anisotropy in the continental lithosphere: A North American case study and global reanalysis

Lara M. Kalnins[a,b,*], Frederik J. Simons[c], Jon F. Kirby[d], Dong V. Wang[e], Sofia C. Olhede[f]

[a]*Department of Earth Sciences, University of Oxford, South Parks Road, Oxford, OX1 3AN, United Kingdom.*
[b]*Department of Earth Sciences, Durham University, Science Labs, Durham, DH1 3LE, United Kingdom.*
[c]*Department of Geosciences, Princeton University, Guyot Hall 321b, Princeton, NJ 08544, U.S.A.*
[d]*Department of Spatial Sciences, Curtin University, GPO Box U1987, Perth 6845, Australia.*
[e]*Department of Statistics and Operations Research, University of North Carolina at Chapel Hill, NC 27599, U.S.A.*
[f]*Department of Statistical Science, University College London, London, WC1E 6BT, United Kingdom.*

Abstract

Lithospheric strength variations both influence and are influenced by many tectonic processes, including orogenesis and rifting cycles. The long, complex, and highly anisotropic histories of the continental lithosphere might lead to a natural expectation of widespread mechanical anisotropy. Anisotropy in the coherence between topography and gravity anomalies is indeed often observed, but whether it corresponds to an elastic thickness that is anisotropic remains in question. If coherence is used to estimate flexural strength of the lithosphere, the null-hypothesis of elastic isotropy can only be rejected when there is significant anisotropy in both the coherence and the elastic strengths derived from it, and if interference from anisotropy in the data themselves can be plausibly excluded. We consider coherence estimates made using multitaper and wavelet methods, from which estimates of effective elastic thickness are derived. We develop a series of statistical and geophysical tests for anisotropy, and specifically evaluate the potential for spurious results with synthetically generated data. Our primary case study, the North American continent, does not exhibit meaningful anisotropy in its mechanical strength. Similarly, a global reanalysis of continental gravity and topography using multitaper methods produces only scant evidence for lithospheric flexural anisotropy.

Keywords: elastic thickness, lithospheric anisotropy, lithospheric flexure, tectonic inheritance, hypothesis testing

1. Introduction

In what are arguably the two most important textbooks published on the subject of flexure and isostasy, neither Lambeck (1988) nor Watts (2001) devotes much space to the question whether the flexural elastic response of the lithosphere might be directionally (azimuthally) anisotropic, and this despite some early evidence (Stephenson and Beaumont, 1980; Stephenson and Lambeck, 1985; Lowry and Smith, 1995) predating the publication of these works. On the other hand, azimuthal anisotropy is hardly ever absent from a discussion of the seismic signature of lithospheric deformation (Silver, 1996; Montagner, 1998; Park and Levin, 2002), and even very long-term, viscous, anisotropy (Honda, 1986; Christensen, 1987; Lev and Hager, 2008; Tommasi et al., 2008; Hansen et al., 2012) enjoys moderate but sustained attention from modellers and experimentalists alike.

The long-term (> 1 Myr) flexural strength of the lithosphere is commonly measured in terms of an effective elastic thickness, T_e, which is related to the rigidity, D, of a perfectly elastic plate by

$$D = \frac{ET_e^3}{12(1-\nu^2)}, \tag{1}$$

where E is Young's modulus and ν is Poisson's ratio, both generally assumed to be constant throughout the lithosphere. In reality, the long-term strength of the lithosphere is a combination of brittle, elastic, and ductile strength; in the case of the continental lithosphere, the compositionally distinct upper crust, lower crust, and lithospheric mantle may each include all three regimes (e.g., Burov and Diament, 1995; Burov, 2010). Rather than corresponding to any specific isotherm or compositional boundary, T_e measures the combined effect of this complex rheology by analogy with a purely elastic plate, whose thickness represents the integrated strength (e.g., Burov, 2010).

Anisotropy in the elastic behaviour is not easily measured; it is difficult to separate from the complexity of resolving the isotropic elastic response. The latter may be estimated using a variety of methods, including forward modelling of seismic (e.g., Watts et al., 1985) or topography and gravity (e.g., Watts et al., 1980) profiles, but continental-scale studies of spatial variation in T_e are most commonly performed via cross-spectral analysis of topography and gravity anomalies (e.g., Dorman and Lewis, 1970; McKenzie and Bowin, 1976; Watts, 1978; Forsyth, 1985), which usually involves admittance or coherence

*Corresponding author at: Department of Earth Sciences, Durham University, Science Labs, Durham, DH1 3LE, United Kingdom. Tel: +44 (0)1913 342347. Email: lara.kalnins@durham.ac.uk.

functions. A variety of statistical devices, such as windowing and tapering, are called upon to diminish the bias and reduce the variance of the estimates (e.g., Ojeda and Whitman, 2002; Crosby, 2007; Kalnins and Watts, 2009; Pérez-Gussinyé et al., 2009). However, the reduction of hundreds of gravity and topography data points to admittance or coherence estimates at a handful of statistically uncorrelated wavenumbers results in a loss of statistical efficiency, limiting the potential of admittance and coherence-based T_e estimates, however well carried out (Simons and Olhede, 2013).

Nevertheless, after the early works cited, increased attention led to the development of a suite of methods to locally extract directional anisotropy in the effective elastic thickness (Simons et al., 2000, 2003; Swain and Kirby, 2003a; Audet and Mareschal, 2004; Kirby and Swain, 2006). First applied to the Australian continent and the Canadian Shield, these methods have since yielded apparent evidence for pervasive mechanical anisotropy worldwide (Rajesh et al., 2003; Stephen et al., 2003; Nair et al., 2011, 2012; Zamani et al., 2013).

Audet and Bürgmann (2011) made a geologically attractive case for tectonic inheritance being a controlling factor in the deformation behaviour of the lithosphere throughout supercontinent cycles. Their analysis, like that of Simons et al. (2000), relied on the identification of weak directions with azimuths where the coherence between Bouguer gravity anomalies and topography exceeds the isotropic average. Finding examples of such anisotropy in the continents worldwide, Audet and Bürgmann (2011) then showed its correlation with lateral gradients in the isotropically-estimated elastic thickness, which are often aligned perpendicular to tectonic boundaries.

In this paper we draw attention to the "lingering problems" and "unresolved question[s]" identified by Audet (2014), indeed, to the general difficulty of inferring lithospheric anisotropy from gravity-topography coherence. We specifically formulate our own concerns that a great many of the "weak" directions marked in Figure 1 of the paper by Audet and Bürgmann (2011), and by implication, in the work of most other workers including some authors of this present study (e.g., Simons et al., 2000, 2003; Kirby and Swain, 2006), may in fact be spurious artefacts due to the statistical properties of the analysis method.

2. Method and Motivation

The coherence γ^2 is a normalised cross-power spectral density S of topography H and gravity G,

$$\gamma^2_{GH}(\mathbf{r},\mathbf{k}) = \frac{|S_{GH}(\mathbf{r},\mathbf{k})|^2}{S_{GG}(\mathbf{r},\mathbf{k})S_{HH}(\mathbf{r},\mathbf{k})}, \tag{2}$$

where $\mathbf{r}$ is the spatial-domain position vector and $\mathbf{k}$ the spectral-domain wave vector. It is a statistical measure of the average wavelength-dependent relation between two multivariate fields (Bendat and Piersol, 2000). That it contains information about the isostatic or flexural compensation mechanism by which to estimate the variable strength of the lithosphere is not in question here (but see Simons and Olhede, 2013). However, the identification of directionally anisotropic behaviour in the estimated coherence between gravity and topography — a methodology that one of us is at least partly responsible for promoting (Simons et al., 2000, 2003) — is not sufficient indication of intrinsic anisotropy in the mechanical process linking both geophysical fields (Swain and Kirby, 2003a; Kirby and Swain, 2006).

Two further basic ingredients are necessary for the conclusion that lithospheric strength behaves anisotropically, i.e. differently depending on the look direction (azimuth). Firstly, it is necessary to establish that the directional variations of the coherence at a given constant wavenumber are robust and statistically significant with non-negligible probability. They should not arise by chance under a null-hypothesis of intrinsically isotropic behaviour, as could be due, for instance, to spectral discretisation effects or when anisotropic initial loads are emplaced on an isotropic lithosphere. Secondly, any robust variations in the coherence must lead to significant anisotropic variations in the parameter of interest, namely, the lithospheric flexural rigidity, which is derived from it by an inversion that is subject to its own, potentially large, estimation uncertainty.

As to the first requirement, it should be shown that when no lithospheric anisotropy is in the system, none is introduced by the analysis. As to the second, the inferred directionally dependent values of elastic strength need to be evaluated against the uncertainty with which the isotropic elastic strength can be determined from the same data. Such a statistical analysis will need to be tailored to the method used to determine the coherence, whether via multitaper spectral analysis, wavelets, or any other method. We can thus greatly reduce spurious identifications via statistical tests on the coherence, on the results of the rigidity estimation, and finally, by testing that it is not simply the widespread spectral anisotropies of gravity or topography themselves which impart apparent anisotropy to the coherence, or apparent anisotropy to the rigidity estimated from their relation.

In order to explore how widespread spurious anisotropy measurements may be in existing studies, we have chosen to test two methods commonly used (with variants) over the last fifteen years: the Slepian-windowed multitaper method (duration $\times$ half-bandwidth product $NW = 3$, Shannon number 6, using 4 tapers in each dimension) of Simons et al. (2000) and the fan-wavelet method (Morlet wavelet with central wavenumber $k_0 = 5.336$) of Kirby and Swain (2006, 2011), which is the basis of the fan-wavelet method of Audet and Mareschal (2007). For simplicity, we use square data patches or windows. Selective methods for regions of arbitrary description, such as irregular tectonic provinces, have also been developed, and may help avoid blending contrasting T_e from different features into a single estimate (Simons and Wang, 2011). However, most workers to date have used square or circular windows, making a simple geometric patch a better test domain for the reliability of existing analyses.

There are a great many subtleties involved in "inverting" a coherence curve for a proper estimate of the effective elastic thickness, including the choice of Bouguer versus free-air gravity anomalies (McKenzie and Fairhead, 1997; Banks

et al., 2001; McKenzie, 2003; Swain and Kirby, 2003b; Pérez-Gussinyé et al., 2004). The difficulties are especially daunting in the presence of correlation (r) between surface and subsurface loading (Macario et al., 1995; McKenzie, 2003; Kirby and Swain, 2009), which are furthermore present in an unknown proportion of variance to each other, the loading ratio (f^2), which may be wavenumber-dependent (Simons and Olhede, 2013). We point to the comprehensive overviews and historical reviews by Simons and Olhede (2013) and Kirby (2014) for more context. Here, for the multitaper method, we use the simple coherence transition-wavelength metric to determine relative values in effective elastic thickness (Simons and van der Hilst, 2002, 2003; Kirby and Swain, 2008b), and for the wavelet results we remain faithful to the method of Kirby and Swain (2006), which was used with some modifications by Audet and Bürgmann (2011). Following the majority of previous anisotropy studies, we use the Bouguer gravity anomaly with both methods.

3. Anisotropy Tests for Coherence and T_e

For our statistical testing, any estimate of the two-dimensional gravity-topography coherence is simply denoted $\gamma^2(\mathbf{k}) = \gamma^2(k,\theta)$. The wave vector $\mathbf{k}$-half-plane is parameterised using an azimuth (θ, quoted from 0 to π, increasing anticlockwise from a bearing of 90° to 270°) and a radius ($k = |\mathbf{k}|$, the wavenumber). The coherence estimate is asymptotically Gaussian (Carter et al., 1973; Touzi and Lopes, 1996; Walden, 1990). The grand average is the constant denoted $\overline{\gamma}^2$. Averaging $\gamma^2(\mathbf{k})$ over all available wavenumbers in a particular direction produces the radially averaged quantity $\overline{\gamma}^2(\theta)$, whereas averaging over all azimuths at a particular wavenumber produces the directionally averaged quantity $\overline{\gamma}^2(k)$. The respective uncertainties are the standard deviations $\sigma_{\gamma^2}(\mathbf{k})$, $\sigma_{\overline{\gamma}^2}(\theta)$, and $\sigma_{\overline{\gamma}^2}(k)$, always written with the explicit functional dependence on $\mathbf{k}$, θ, or k, where applicable.

For multitaper estimates made as discussed by Simons et al. (2003), with J Slepian tapers, the standard deviation of the coherence is taken to be the square root of $\sigma^2_{\gamma^2}(\mathbf{k}) = 2\gamma^2(\mathbf{k})\Big[1-\gamma^2(\mathbf{k})\Big]^2/J$. Other scale estimates for the coherence may be substituted (e.g., Chave et al., 1987), but from any $\sigma^2_{\gamma^2}(\mathbf{k})$ we obtain, by averaging, $\sigma^2_{\overline{\gamma}^2}(\theta) = N^{-2}_{k(\theta)} \sum_{k(\theta)} \sigma^2_{\gamma^2}(k,\theta)$, and $\sigma^2_{\overline{\gamma}^2}(k) = N^{-2}_{\theta(k)} \sum_{\theta(k)} \sigma^2_{\gamma^2}(k,\theta)$, where the sums are over the $N_{k(\theta)}$ or $N_{\theta(k)}$ gridded positions $k(\theta)$ or $\theta(k)$ defined on a subgrid of wave vectors (k,θ) that are separated by half the taper bandwidth. At that set of wavenumbers the coherence estimates can be considered sufficiently uncorrelated according to standard Slepian-multitaper theory (Percival and Walden, 1993) and its extensions (Dahlen and Simons, 2008; Kirby and Swain, 2013; Simons and Olhede, 2013), which motivates our variance calculation of $\sigma^2_{\overline{\gamma}^2}(\theta)$ and $\sigma^2_{\overline{\gamma}^2}(k)$.

3.1. Test for Mathematical Significance

Our first test is for "mathematical significance": whether the coherence itself is significantly anisotropic. To illustrate, Figure 1a shows a coherence estimate, $\gamma^2(k,\theta)$, made at a location in the Labrador Sea and displaying visible anisotropy. Figure 1b then compares the radial average $\overline{\gamma}^2(\theta)$ with the grand average $\overline{\gamma}^2$. Because we are ultimately looking for robust directions, we also use a scaled threshold to define the angular resolution of the identified peaks, the azimuthal range over which

$$|\overline{\gamma}^2(\theta) - \overline{\gamma}^2(\theta_e)| < \sigma_{\overline{\gamma}^2}(\theta) + \sigma_{\overline{\gamma}^2}(\theta_e), \tag{3}$$

where θ_e is the azimuth of the extremum. A positive identification for mathematically significant anisotropy is made when (1) the local extremum of the radially averaged coherence, $\overline{\gamma}^2(\theta)$, is separated from the mean coherence, $\overline{\gamma}^2$, by more than $2\sigma_{\overline{\gamma}^2}(\theta)$ and (2) the angular resolution of the peak is sharper than 60°. In the case shown in Figure 1b, both the maximum and minimum pass the significance and width tests, but no secondary extrema do.

3.2. Test for Geophysical Significance

Our second test is one of "geophysical significance": whether the anisotropy in the coherence translates into a resolvable anisotropy in flexural strength. Is the anisotropy in the wavelengths sensitive to T_e, and does it exceed the uncertainty associated with the inversion? The first criterion is that the coherence provide a good match to Forsyth's (1985) model of uncorrelated surface and subsurface loading, under which we expect high coherence (> 0.75) at long wavelengths and low coherence (< 0.5) at short ones, with a well-defined transition wavelength separating both regimes (see the "Standard Model" as discussed by Simons and Olhede, 2013). We can then use the simplest possible route to "convert" a coherence measurement to an effective elastic thickness, by ignoring load correlations ($r = 0$), assuming a fixed constant loading ratio $f^2 = 0.5$, and analytically solving for the T_e that corresponds to the observed half-coherence wavenumber $k_{1/2}$, where $\gamma^2 = 1/2$ (Simons and van der Hilst, 2002, 2003; Kirby and Swain, 2008a,b; Simons and Olhede, 2013).

This method minimises the effect of short-wavelength anisotropy on our estimate of T_e, and provides a simple measure of its uncertainty based on the uncertainty in the wavenumber from which it is estimated (half the taper bandwidth, as discussed earlier in Section 3). Due to the underlying (and not uncommon) assumptions about f^2 and r, we cannot place much faith on the absolute determination of the T_e using this method. However, our focus here is on directional variation, rather than absolute value. Since the spatial regions we compare are of equal size, and f^2 and r should in most cases be relatively slowly varying and thus reasonably constant within a region, we should still be able detect anisotropy in T_e. It is possible, however, that a sharp gradient in r or f^2 could be wrongly detected as flexural anisotropy rather than a change in loading; the tradeoff between f^2 and T_e, in particular, is a well-known and ubiquitous challenge in estimating T_e from coherence (e.g., Banks et al., 2001; McKenzie, 2003; Simons and Olhede, 2013).

Returning to our worked example, the black circle in Figure 1a marks the "half-point" of the azimuthally averaged coherence; its wavelength, $\lambda_{1/2} = 2\pi/k_{1/2}$, is given in km in the

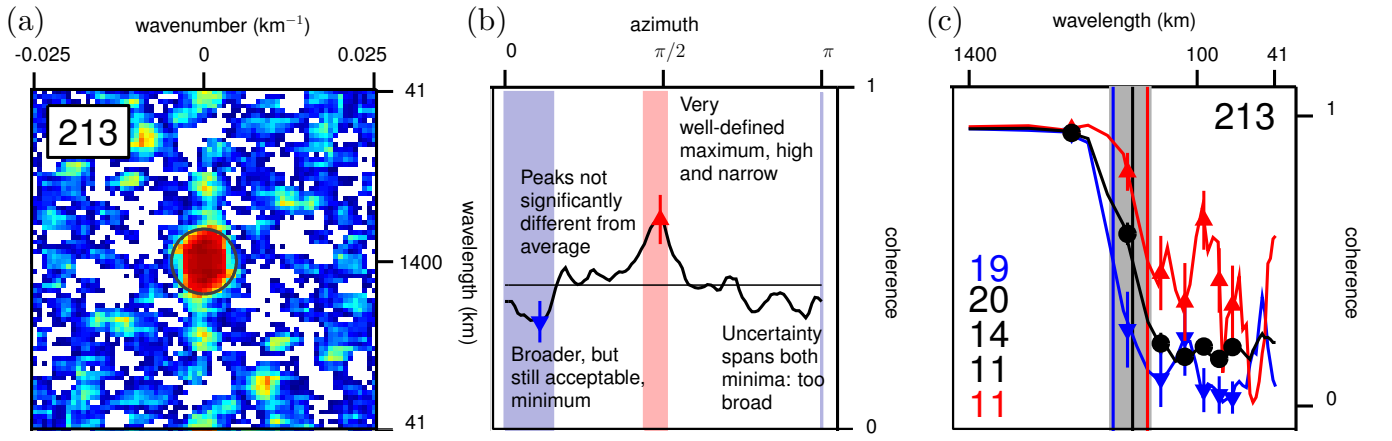

Figure 1: Testing coherence and elastic thickness estimates for anisotropy: real data example. All error bars shown are plus/minus two standard deviations. (a) An example with visible anisotropy in the north-south direction. The azimuthally averaged coherence reaches 0.5 at a wavelength of 213 km, marked by the black circle. Values below 0.1 left white. (b) Mean coherence (averaged over azimuth and wavenumber; horizontal black line), and radially averaged coherence (a function of azimuth; thick black curve), with red and blue triangles indicating the global maximum and minimum. Shading defines ranges of significant and well-resolved anisotropy, in this case around one directional low (blue) and one high (red) in the coherence. (c) Azimuthally averaged coherence (a function of wavenumber; black), with filled symbols showing approximately statistically uncorrelated wavenumbers. Coherence in the directions of the maximum (red), and minimum radially averaged coherence (blue). Vertical lines mark the half-points of the curves. Grey band marks the wavenumber uncertainty of the azimuthally averaged (black) half-points. As in (a), 213 is the wavelength of the half-point. The directional T_e estimates are 19 km (from the blue curve) and 11 km (from the red curve). The T_e estimate from the isotropic average (black curve) is 14 km with lower and upper bounds of 11 km and 20 km. As the isotropic bounds exceed the directional estimates, there is no robust indication of anisotropy in the effective elastic thickness.

upper left. Figure 1c shows the azimuthally averaged coherence $\overline{\gamma}^2(k)$ as a thick black curve, with the half-point marked as a vertical line. This is contrasted with the curves $\gamma^2(k, \theta_e)$ retrieved in the directions θ_e of the maximum (red) and minimum (blue) that were retained by the analysis of the radially averaged coherence $\overline{\gamma}^2(\theta)$ shown in Figure 1b. The vertical lines show the half-point of each curve, with the corresponding T_e values shown in the lower left, and we can see that the half-points for the anisotropic extrema fall within the uncertainty of the isotropic estimate, indicated by the grey band. Thus, despite the coherence anisotropy being mathematically significant, neither the derived maximum nor the minimum lithospheric anisotropy is geophysically significant and our example does not robustly indicate anything that can be interpreted as actual anisotropy in lithospheric strength.

3.3. Test for Bias from Anisotropy in Gravity or Topography

Our third test aims to remove the potential anisotropic bias introduced to the coherence from analysing intrinsically anisotropic fields such as topography and gravity: anisotropies in the power-spectral densities of the individual fields H and G themselves may impart anisotropy to the coherence estimate, even when the intrinsic behaviour of the lithosphere is isotropic (Simons and Olhede, 2013; Kirby, 2014). To illustrate, Figure 2a shows estimates of the power-spectral density of the topography in the North American continent, formed over 25 non-overlapping square (1400 km on the side) patches. Substantial anisotropy is visible to the untrained eye. We map the anisotropy in topography and gravity over the continent via a radially-averaged azimuthal significance analysis, as shown for the coherence in Figure 1b. Figure 2b then shows how significant directional extrema in topography and gravity align with those in the coherence.

Where the directions are clearly aligned, we must consider whether the apparent anisotropy in T_e is purely an artefact of the anisotropy in topography or gravity. We consider the directions aligned if the azimuthal ranges for coherence and gravity/topography overlap; however, for clarity, the azimuthal ranges for gravity and topography are not shown in Figure 2b. Across the 25 patches shown, four directions will be rejected. However, in many geological settings, genuine lithospheric weakness may be aligned with structures in the topography/gravity. We have deliberately performed this test last to facilitate consideration of this possibility. (See the figures on azimuthal bias in the Supplementary Material for details.)

4. Synthetic Tests, Multitapers, and Wavelets

To test the coherence estimation methods currently widely used as well as our proposed significance testing, we perform anisotropy analysis on two types of synthetic data, one wholly synthetic and the other using the actual topography of North America. For the first, we use the method of Simons and Olhede (2013), who developed a procedure to generate synthetic gravity and topography fields that are jointly isotropic and coupled via an intrinsically isotropic flexural equation. Their method assumes a stationary isotropic Matérn spectral form (Handcock and Wallis, 1994; Guttorp and Gneiting, 2006) for the initial surface and subsurface loads, which are simulated in known proportion (constant f^2) and correlation (constant r) to each other. The only other parameters in the model are the flexural rigidity D, related to T_e by equation 1, the depth to the subsurface interface z_2, and the density contrasts Δ_1 and Δ_2 across the surface and subsurface interfaces. No aspect of the model is anisotropic in any way.

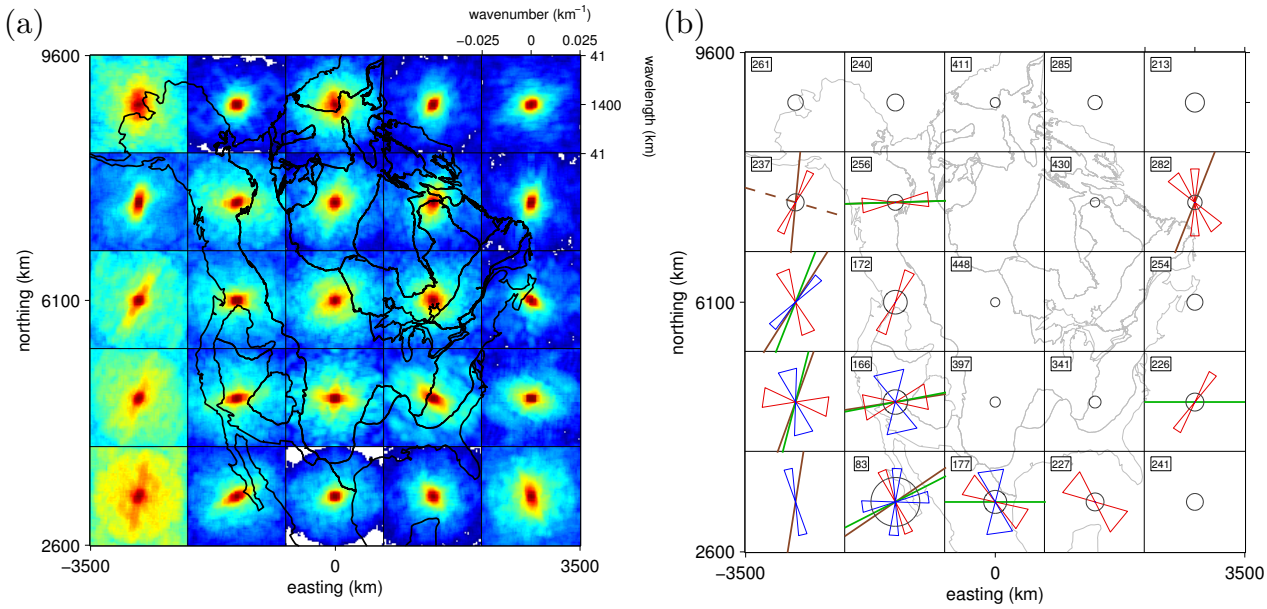

Figure 2: Possible bias in the coherence anisotropy from topography or gravity anisotropy and summary of the continent-wide analysis for mechanical anisotropy. (a) Power spectral density of North American topography from the EGM2008 model (Pavlis et al., 2012), analysed in 1400 × 1400 km non-overlapping patches. Geological province boundaries are after Vigil et al. (2000). (b) Mechanical anisotropy in the North American lithosphere analysed from topography and Bouguer gravity over the same 25 windows shown in (a). Black circles identify azimuthally-averaged coherence half-points, and boxed numbers their corresponding wavelengths in km, as in Figure 1a. Red and blue wedges show azimuthal ranges of (high and low, respectively) coherence anisotropy that pass both the mathematical (Figure 1b) and geophysical (Figure 1c) significance tests. Brown and green lines indicate significant maxima (solid lines) and minima (dashed lines) in the radially averaged power spectral density of the topography and Bouguer gravity anomaly, respectively. No values or measurements are plotted when the measurements are deemed insufficiently well determined.

Our second set of synthetic data uses the method of Kirby and Swain (2009), who developed a scheme to generate synthetic gravity anomaly data from observed topography, in a similar two-layer setup with an isotropic flexural rigidity. To simulate data under an uncorrelated initial-loading scenario, their synthetics are the average of 100 Bouguer anomalies calculated from 100 fractally simulated (Swain and Kirby, 2003b) initial surface loads together with the observed topography, thereby averaging out random instances of load correlation (Kirby and Swain, 2008a). In their synthetics, any anisotropy present in the system is solely that which arises from the match to the observed topography, which of course is usually anisotropic. Being characterised by a single D, the lithospheric response itself is wholly isotropic.

We perform anisotropy analysis on these two types of synthetic data over an area the size of North America, using the actual North American topography for the second method. For the multitaper method, hypothesis testing for anisotropy, as in Figures 1 and 2, is performed. For the wavelet analysis, no hypothesis testing is performed *per se*, although the strength of anisotropy is reported as $1 - (T_{\min}/T_{\max})$, which captures the strength of anisotropy of an orthotropic plate as proposed by Swain and Kirby (2003b) and Kirby and Swain (2006). It is the latter analysis that best compares to the procedure followed by Audet and Bürgmann (2011).

What we should expect to see in order to validate our statistical treatment is that our hypothesis testing on the multitaper results successfully rejects any anisotropy in the synthetics. What we fear to see, and what would signal significant concern about the validity of many of the results of previous studies, is widespread anisotropy in the synthetic multitaper results prior to the hypothesis testing proposed here, and in the synthetic wavelet results, for which dedicated wavelet hypothesis tests to rule it out remain in need of development.

Figure 3 summarises the results of the Slepian multitaper analysis (after hypothesis testing for mathematical significance, a and c), and of the fan wavelet analysis (b and d) of the synthetics. Clearly, anisotropy is detectably present in the observed coherence, despite no anisotropy whatsoever present in the mechanical model of the lithosphere. For the multitaper method, much spurious anisotropy survives this first test, but after geophysical significance testing (as in Figure 1c), 100% and 58% of the directions from Figure 3a and c, respectively, are successfully flagged as spurious. As with all statistical tests of the kind, the Type I error of multiple testing is formally set by the significance level (Bendat and Piersol, 2000), with additional tests increasing the number of false positives (Davison, 2003), but here we must recognise that our choices are largely empirical. Adding the bias test for alignment with anisotropy in the gravity or topography rejects a further 31% of the anisotropy in Figure 3c, for a total of 89% identified as spurious. Although genuine alignments between anisotropy in T_e and in gravity/topography may occur in real data, without this criterion, a substantial percentage of the spurious weak directions shown in Figure 3c were retained when testing the Kirby and Swain (2009) synthetics (42%, as opposed to 11% using this criterion); we cannot at present be confident that directions aligned like this are robust.

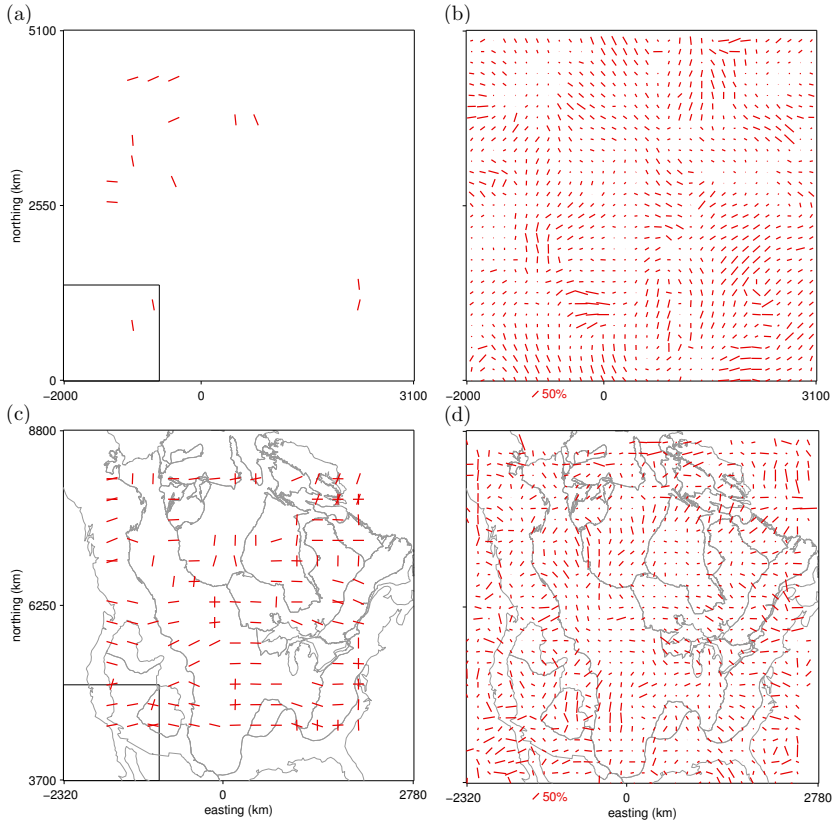

Figure 3: Testing coherence and elastic thickness estimates for mathematically significant anisotropy: synthetic data example. Directions show maxima in the coherence, which correspond to minima in T_e. (a) and (b) show results using Simons and Olhede (2013) synthetics analysed using multitaper and fan-wavelet methods, respectively. (c) and (d) show the corresponding results for the Kirby and Swain (2009) synthetics. For the multitaper method, results are shown after mathematical significance testing, and the window size of 1400 km is shown in the lower left. In the fan-wavelet results, the spatial domain of signal extraction scales inversely with the wavenumber and the length of the bars is scaled to the purported strength of the lithospheric anisotropy. All of the anisotropy is spurious. Of the anisotropy in (a) and (c), 100% of that in (a) and 89% of that in (c) is later identified and removed by the geophysical significance and topography/gravity bias tests.

Hence, judicious use of hypothesis testing would allow us to retain the null-hypothesis of lithospheric intrinsic isotropy in the vast majority of those cases analysed by the multitaper method. However, even after this stringent testing, some spurious anisotropy remains, and results must thus be interpreted with caution. The fan-wavelet results paint a more worrying picture: while they have not been made subject to the hypothesis testing discussed for multitapers, without such testing, much of what is observed in Figures 3b and 3d could be wrongly ascribed to intrinsic lithospheric anisotropy when, in actuality, there is none.

5. The Case of North America

We now consider the elastic anisotropy results using real data for the case of North America. Figure 4a and 4b show the data: topography and Bouguer gravity anomaly, both derived from the EGM2008 release (Pavlis et al., 2012), in a Lambert conformal conic projection. Figure 4c, 4d, and 4e show the results from the statistical analysis of the gravity-topography coherence, conducted on a grid of overlapping 1400×1400 km analysis boxes. Testing only for mathematical significance leaves a great number of anisotropic directions (Figure 4c) but most of those are later rejected by the tests for geophysical significance (Figure 4d) and then for potential bias from anisotropy in the topography or the gravity (Figure 4e). As far as the continental landmass is concerned, almost no evidence for lithospheric anisotropy remains to be interpreted at this scale. Changing the window size to 2500×2500 km (Figure 5a and 5b) and to 3500×3500 km (Figure 5c and 5d) brings out more lithospheric anisotropy, but at those resolutions, the primary generator for the signal could very well be related to the ocean-continent transition or even to anisotropy in the oceanic, rather than continental, lithosphere. Similar analyses for the other continents can be found in the Supplementary Material.

6. Discussion and Conclusions

Lithospheric strength variations play a role in modulating many Earth processes, including large-scale tectonic processes such as rifting and orogeny. These processes in turn are expected to alter the strength of the lithosphere involved. Many geological materials are highly anisotropic, from the crystal to the continental scale, but the effective length scale over which

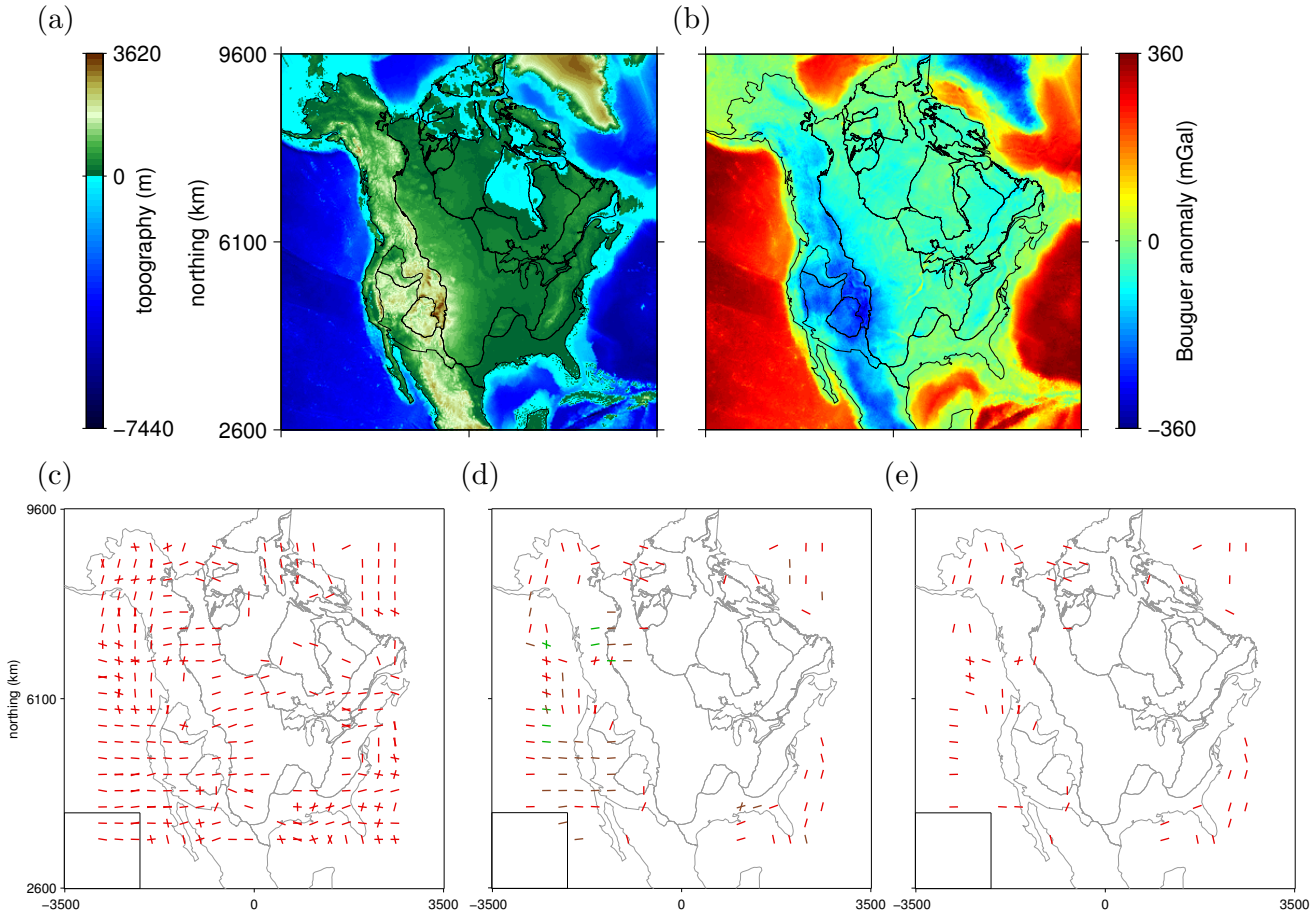

Figure 4: North American topography, gravity, and mechanical anisotropy from directional coherence analysis. (a) Topography and (b) Bouguer gravity anomaly from the EGM2008 model (Pavlis et al., 2012); the Bouguer anomaly is calculated from the model using the infinite-slab method with a crustal density of 2670 kg/m^3 and a mantle density of 3300 kg/m^3. (c) Mathematically significant weak directions detected with a square window size of 1400 km. (d) Weak directions surviving mathematical and geophysical significance testing. Directions aligned with gravity or topography are shown in green or brown, respectively. (e) Weak directions surviving mathematical, geophysical, and bias testing.

anisotropic behaviour exerts a dominant influence will be variable depending on the process under consideration. If no one direction dominates, a combination of varying anisotropies at different scales will also produce an isotropic response. While the natural expectation might be for anisotropy in many locations, a null hypothesis of isotropy should be our point of departure.

It has generally been difficult to relate measurements of lithospheric elastic anisotropy with other measures of anisotropic behaviour in the lithosphere. Concerns about the robustness of the measurements themselves have led to the realisation that anisotropy in the gravity-topography coherence cannot easily be identified with evidence for anisotropy in the mechanical strength of the lithosphere itself. In this paper, we have used synthetic data to reveal that much apparent, but spurious, anisotropy can arise from the analysis method. We have developed a methodology to test the mathematical and geophysical robustness of mechanical anisotropy measurements.

Such spurious anisotropy can arise from many sources. These range from the numerical effects of data gridding and windowing (which is seen very clearly by studying completely isotropic synthetics), to the imprints of anisotropy in the gravity or topography on the coherence (as we have seen in the synthetic studies that used actual topography), and to correlations in the initial loading topographies (which we did not model here) which could be anisotropic. Even the high gradients in the isotropic T_e, which have been suspected by some to be correlated with lithospheric anisotropy, may increase the uncertainty of the measurement. In such a case the data inside a particular window may incorporate a wide range of T_e, thereby increasing how anisotropic a measurement can appear without reflecting intrinsic flexural anisotropy (Kirby, 2014). Even our stringent testing may fail to detect this type of spurious anisotropy. Finally, the complexity and variety of the geological processes linking gravity and topography in the data is likely greater than in the simple linear models by which we relate them, leaving other potentially anisotropic contributions to the coherence unmodelled.

Areas of very high T_e are also locations where apparently highly anisotropic measurements may be within error of the isotropic measurement. Near major geological boundaries and orogenic zones, many of these confounding factors are con-

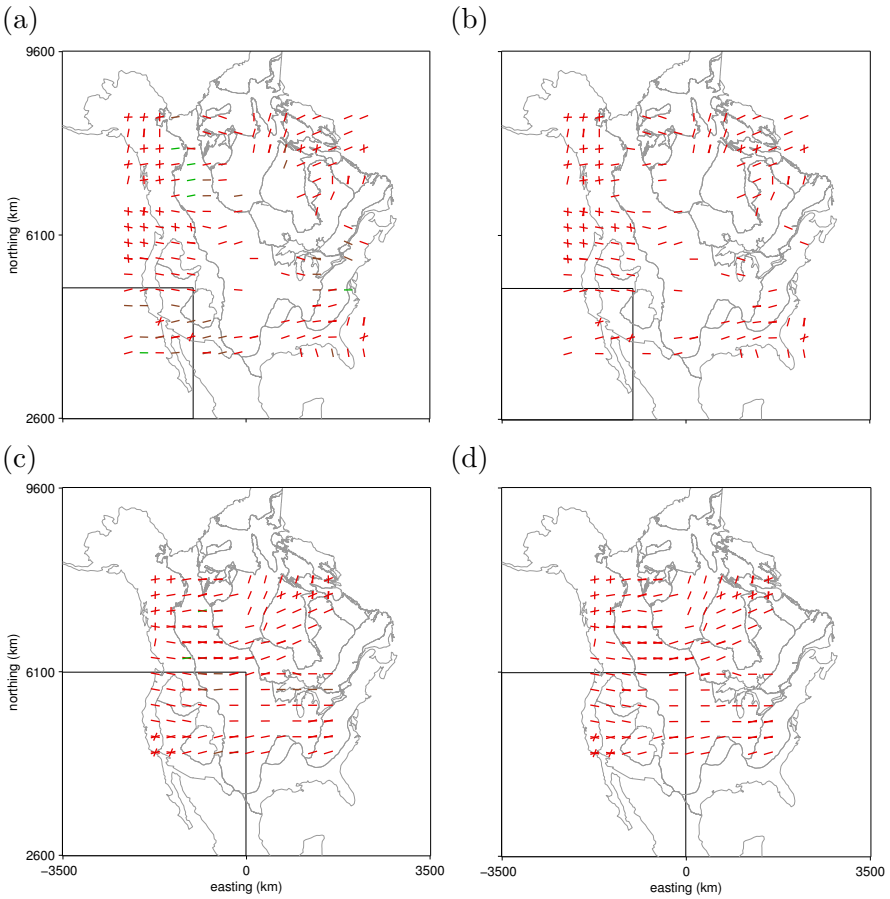

Figure 5: Weak directions surviving mathematical and geophysical significance testing (a and c) and all three tests (b and d), as in Fig. 4d and e, respectively, but with window sizes of (a–b) 2500 km and (c–d) 3500 km.

flated: anisotropic input data, high T_e gradients, as well as many possible sources of legitimate anisotropy in the mechanical strength of the lithosphere itself. Our analysis in no way rules out the possibility that strength in these areas is significantly anisotropic and that this anisotropy plays a major role in large-scale tectonic cycles. However, as also shown in the results of Kirby (2014), it does mean that teasing out and verifying such anisotropy is much more difficult, if not impossible, regardless of the cross-spectral methods being used.

In the absence of solid evidence to the contrary, we must fail to reject the null hypothesis of isotropy. Using the observed coherence between topography and gravity anomalies to model flexural strength of the lithosphere, the null-hypothesis of elastic isotropy should only be rejected when both the coherence itself is significantly anisotropic and the inversions based on the coherence yield significantly anisotropic elastic strengths. In addition, directions aligned with significant anisotropy in the topography or gravity data may also be spurious. A conservative global reanalysis of gravity-topography coherence on these terms, which we present in the Supplementary Material, produces only scant evidence for lithospheric flexural anisotropy, in marked contrast to previous results (Rajesh et al., 2003; Stephen et al., 2003; Nair et al., 2011, 2012; Zamani et al., 2013). We draw attention particularly to the results reported by Audet and Bürgmann (2011), which we feel are in danger of being over-interpreted.

7. Author contributions

LMK, FJS, and DVW designed the study, performed the multitaper analysis and conducted the anisotropy hypothesis testing. JFK designed and performed the wavelet synthetic modelling and coherence anisotropy analysis. FJS and SCO designed and carried out the synythetic data generation and statistical modeling. LMK and FJS designed and produced the figures and wrote the paper. All authors discussed the results and commented on the manuscript.

8. Acknowledgments

This research was partially supported by NSF grants EAR-0710860 and EAR-1150145 and NASA grant NNX11AQ45G to FJS, ARC grant number DP0878453 to JFK, EPSRC Leadership Fellowship EP/I005250/1 and EPSRC grant EP/L001519/1 to SCO, and NERC grant NE/I026839/1, which supported LMK. LMK and JFK thank Princeton University for its support and hospitality. We thank Cindy Ebinger and an anonymous reviewer for their helpful comments.

9. References

Audet, P., 2014. Toward mapping the effective elastic thickness of planetary lithospheres from a spherical wavelet analysis of gravity and topography. Phys. Earth Planet. Inter. 226, 48–82, doi: 10.1016/j.pepi.2013.09.01.

Audet, P., Bürgmann, R., 2011. Dominant role of tectonic inheritance in supercontinent cycles. Nature Geosci. 4 (3), 184–187, doi: 10.1038/ngeo1080.

Audet, P., Mareschal, J.-C., 2004. Anisotropy of the flexural response of the lithosphere in the Canadian Shield. Geophys. Res. Lett. 31, L20601, doi: 10.1029/2004GL021080.

Audet, P., Mareschal, J.-C., 2007. Wavelet analysis of the coherence between Bouguer gravity and topography: application to the elastic thickness anisotropy in the Canadian Shield. Geophys. J. Int. 168, 287–298, doi: 10.1111/j.1365–246X.2006.03231.x.

Banks, R. J., Francis, S. C., Hipkin, R. G., 2001. Effects of loads in the upper crust on estimates of the elastic thickness of the lithosphere. Geophys. J. Int. 145 (1), 291–299.

Bendat, J. S., Piersol, A. G., 2000. Random data: Analysis and measurement procedures, 3rd Edition. John Wiley, New York.

Burov, E. B., 2010. The equivalent elastic thickness (T_e), seismicity and the long-term rheology of continental lithosphere: Time to burn-out "crème brûlée"? Insights from large-scale geodynamic modeling. Tectonophysics 484 (1), 4–26, doi: 10.1016/j.tecto.2009.06.013.

Burov, E. B., Diament, M., 1995. The effective elastic thickness (T_e) of continental lithosphere: What does it really mean? J. Geophys. Res. 100 (B3), 3905–3927.

Carter, G. C., Knapp, C. H., Nuttal, A. H., 1973. Statistics of the estimate of the magnitude-coherence function. IEEE Trans. Audio Electroacoust. AU21, 388–389.

Chave, A. D., Thomson, D. J., Ander, M. E., 1987. On the robust estimation of power spectra, coherences, and transfer functions. J. Geophys. Res. 92 (B1), 633–648.

Christensen, U. R., 1987. Some geodynamical effects of anisotropic viscosity. Geophys. J. R. Astron. Soc. 91 (3), 711–736, doi: 10.1111/j.1365–246X.1987.tb01666.x.

Crosby, A. G., 2007. An assessment of the accuracy of admittance and coherence estimates using synthetic data. Geophys. J. Int. 171 (1), 25–54.

Dahlen, F. A., Simons, F. J., 2008. Spectral estimation on a sphere in geophysics and cosmology. Geophys. J. Int. 174, 774–807, doi: 10.1111/j.1365–246X.2008.03854.x.

Davison, A. C., 2003. Statistical Models. Cambridge Univ. Press, Cambridge, UK.

Dorman, L. M., Lewis, B. T. R., 1970. Experimental isostasy, 1, Theory of the determination of the Earth's isostatic response to a concentrated load. J. Geophys. Res. 75 (17), 3357–3365.

Forsyth, D. W., 1985. Subsurface loading and estimates of the flexural rigidity of continental lithosphere. J. Geophys. Res. 90 (B14), 12623–12632.

Guttorp, P., Gneiting, T., 2006. Studies in the history of probability and statistics XLIX. On the Matérn correlation family. Biometrika 93 (4), 989–995.

Handcock, M. S., Wallis, J. R., 1994. An approach to statistical spatial-temporal modeling of meteorological fields. J. Acoust. Soc. Am. 89 (426), 368–378.

Hansen, L. N., Zimmerman, M. E., Kohlstedt, D. L., 2012. Laboratory measurements of the viscous anisotropy of olivine aggregates. Nature 492, 415–418, doi: 10.1038/nature11671.

Honda, S., 1986. Strong anisotropic flow in a finely layered asthenosphere. Geophys. Res. Lett. 13 (13), 1454–1457, doi: 10.1029/GL013i013p01454.

Kalnins, L. M., Watts, A. B., 2009. Spatial variations in effective elastic thickness in the Western Pacific Ocean and their implications for Mesozoic volcanism. Earth Planet. Sci. Lett. 286 (1–2), 89–100, doi: 10.1016/j.epsl.2009.06.018.

Kirby, J. F., 2014. Estimation of the effective elastic thickness of the lithosphere using inverse spectral methods: The state of the art. Tectonophysics 631, 87–116, 10.1016/j.tecto.2014.04.021.

Kirby, J. F., Swain, C. J., 2006. Mapping the mechanical anisotropy of the lithosphere using a 2D wavelet coherence, and its application to Australia. Phys. Earth Planet. Inter. 158 (2–4), 122–138, doi: 10.1016/j.pepi.2006.03.022.

Kirby, J. F., Swain, C. J., 2008a. An accuracy assessment of the fan wavelet coherence method for elastic thickness estimation. Geochem. Geophys. Geosys. 9 (3), Q03022, doi: 10.1029/2007GC001773.

Kirby, J. F., Swain, C. J., 2008b. Correction to "An accuracy assessment of the fan wavelet coherence method for elastic thickness estimation". Geochem. Geophys. Geosys. 9 (5), Q05021, doi: 10.1029/2008GC002071.

Kirby, J. F., Swain, C. J., 2009. A reassessment of spectral T_e estimation in continental interiors: The case of North America. J. Geophys. Res. 114 (B8), B08401, doi: 10.1029/2009JB006356.

Kirby, J. F., Swain, C. J., 2011. Improving the spatial resolution of effective elastic thickness estimation with the fan wavelet transform. Comput. Geosc. 37 (9), 1345–1354, doi: 10.1016/j.cageo.2010.10.008.

Kirby, J. F., Swain, C. J., 2013. Power spectral estimates using two-dimensional Morlet-fan wavelets with emphasis on the long wavelengths: jackknife errors, bandwidth resolution and orthogonality properties. Geophys. J. Int. 194, 78–99, doi: 10.1093/gji/ggt103.

Lambeck, K., 1988. Geophysical Geodesy. Oxford Univ. Press, New York.

Lev, E., Hager, B. H., 2008. Rayleigh-Taylor instabilities with anisotropic lithospheric viscosity. Geophys. J. Int. 173 (3), 806–814, doi: 10.1111/j.1365–246X.2008.03731.x.

Lowry, A. R., Smith, R. B., 1995. Strength and rheology of the western U. S. Cordillera. J. Geophys. Res. 100 (B9), 17947–17963.

Macario, A., Malinverno, A., Haxby, W. F., 1995. On the robustness of elastic thickness estimates obtained using the coherence method. J. Geophys. Res. 100 (B8), 15163–15172.

McKenzie, D., 2003. Estimating T_e in the presence of internal loads. J. Geophys. Res. 108 (B9), 2348, doi: 10.1029/2002JB001766.

McKenzie, D. P., Bowin, C., 1976. The relationship between bathymetry and gravity in the Atlantic Ocean. J. Geophys. Res. 81 (11), 1903–1915.

McKenzie, D. P., Fairhead, J. D., 1997. Estimates of the effective elastic thickness of the continental lithosphere from Bouguer and free air gravity anomalies. J. Geophys. Res. 102 (B12), 27523–27552.

Montagner, J.-P., 1998. Where can seismic anisotropy be detected in the Earth's mantle? In boundary layers... Pure Appl. Geophys. 151 (2–4), 223–256, doi: 10.1007/s000240050113.

Nair, R. R., Majo, T. K., Mati, T., Kandpal, S. C., Kumar, R. T. R., Shekhar, S., 2011. Multitaper coherence method for appraising the elastic thickness of the Indonesian active continental margin. J. Asian Earth Sci. 40, 326–333, doi: 10.1016/j.jseaes.2010.06.009.

Nair, R. R., Singh, Y., Trivedi, D., Kandpal, S. C., 2012. Anisotropy in the flexural response of the Indian Shield. Tectonophysics 532–535, doi: 193–204, doi: 10.1016/j.tecto.2012.02.006.

Ojeda, G. Y., Whitman, D., 2002. Effect of windowing on lithosphere elastic thickness estimates obatined via the coherence method: Results from northern South America. J. Geophys. Res. 107 (B11), 2275, doi: 10.1029/2000JB000114.

Park, J., Levin, V., 2002. Seismic anisotropy: Tracing plate dynamics in the mantle. Science 296, 485–489.

Pavlis, N. K., Holmes, S. A., Kenyon, S. C., Factor, J. K., 2012. The development and evaluation of the Earth Gravitational Model 2008 (EGM2008). J. Geophys. Res. 117, B04406, doi:10.1029/2011JB008916.

Percival, D. B., Walden, A. T., 1993. Spectral analysis for physical applications, multitaper and conventional univariate techniques. Cambridge Univ. Press, New York.

Pérez-Gussinyé, M., Lowry, A., Watts, A. B., Velicogna, I., 2004. On the recovery of effective elastic thickness using spectral methods: Examples from synthetic data and from the Fennoscandian Shield. J. Geophys. Res. 109, B10409, doi: 10.1029/2003JB002788.

Pérez-Gussinyé, M., Swain, C. J., Kirby, J. F., Lowry, A. R., 2009. Spatial variations of the effective elastic thickness, T_e, using multitaper spectral estimation and wavelet methods: Examples from synthetic data and application to South America. Geochem. Geophys. Geosys. 10 (4), Q04005, doi: 10.1029/2008GC002229.

Rajesh, R. S., Stephen, J., Mishra, D. C., 2003. Isostatic response and anisotropy of the Eastern Himalayan-Tibetan Plateau: A reappraisal using multitaper spectral analysis. Geophys. Res. Lett. 30 (2), 1060, doi: 10.1029/2002GL016104.

Silver, P. G., 1996. Seismic anisotropy beneath the continents: Probing the depths of geology. Annu. Rev. Earth. Planet. Sc. 24, 385–432.

Simons, F. J., Olhede, S. C., 2013. Maximum-likelihood estimation of lithospheric flexural rigidity, initial-loading fraction, and load correlation, under isotropy. Geophys. J. Int. 193 (3), 1300–1342, doi: 10.1093/gji/ggt056.

Simons, F. J., van der Hilst, R. D., 2002. Age-dependent seismic thickness and mechanical strength of the Australian lithosphere. Geophys. Res. Lett.

29 (11), 1529, doi: 10.1029/2002GL014962.

Simons, F. J., van der Hilst, R. D., 2003. Seismic and mechanical anisotropy and the past and present deformation of the Australian lithosphere. Earth Planet. Sci. Lett. 211 (3–4), 271–286, doi: 10.1016/S0012–821X(03)00198–5.

Simons, F. J., van der Hilst, R. D., Zuber, M. T., 2003. Spatiospectral localization of isostatic coherence anisotropy in Australia and its relation to seismic anisotropy: Implications for lithospheric deformation. J. Geophys. Res. 108 (B5), 2250, doi: 10.1029/2001JB000704.

Simons, F. J., Wang, D. V., 2011. Spatiospectral concentration in the Cartesian plane. Intern. J. Geomath. 2 (1), 1–36, doi: 10.1007/s13137–011–0016–z.

Simons, F. J., Zuber, M. T., Korenaga, J., 2000. Isostatic response of the Australian lithosphere: Estimation of effective elastic thickness and anisotropy using multitaper spectral analysis. J. Geophys. Res. 105 (B8), 19163–19184, doi: 10.1029/2000JB900157.

Stephen, J., Singh, S. B., Yedekar, D. B., 2003. Elastic thickness and isostatic coherence anisotropy in the South Indian Peninsular Shield and its implications. Geophys. Res. Lett. 30 (16), 1853, doi: 10.1029/2003GL017686.

Stephenson, R., Beaumont, C., 1980. Small-scale convection in the upper mantle and the isostatic response of the Canadian shield. In: Davies, P. A., Runcorn, S. K. (Eds.), Mechanisms of Continental Drift and Plate Tectonics. Academic Press, San Diego, Calif., pp. 111–122.

Stephenson, R., Lambeck, K., 1985. Isostatic response of the lithosphere with in-plane stress: Application to central Australia. J. Geophys. Res. 90 (B10), 8581–8588, doi: 10.1029/JB090iB10p08581.

Swain, C. J., Kirby, J. F., 2003a. The coherence method using a thin anisotropic elastic plate model. Geophys. Res. Lett. 30 (19), 2014, doi: 10.1029/2003GL018350.

Swain, C. J., Kirby, J. F., 2003b. The effect of "noise" on estimates of the elastic thickness of the continental lithopshere by the coherence method. Geophys. Res. Lett. 30 (11), 1574, doi: 10.1029/2003GL017070.

Tommasi, A., Knoll, M., Vauchez, A., Signorelli, J. W., Thoraval, C., Logé, R., 2008. Structural reactivation in plate tectonics controlled by olivine crystal anisotropy. Nature Geosci. 2, 423–427, doi: 10.1038/ngeo528.

Touzi, R., Lopes, A., 1996. Statistics of the Stokes parameters and of the complex coherence parameters in one-look and multilook speckle fields. IEEE Trans. Geosci. Remote Sens. 34 (2), 519–531.

Vigil, J. F., Pike, R. J., Howell, D. G., 2000. A tapestry of time and terrain. Investigations Series 2720, United States Geological Survey, `http://pubs.usgs.gov/imap/i2720/`.

Walden, A. T., 1990. Maximum likelihood estimation of magnitude-squared multiple and ordinary coherence. Signal Process. 19, 75–82.

Watts, A. B., 1978. An analysis of isostasy in the world's oceans, 1, Hawaiian-Emperor seamount chain. J. Geophys. Res. 83 (B12), 5989–6004.

Watts, A. B., 2001. Isostasy and Flexure of the Lithosphere. Cambridge Univ. Press, Cambridge, UK.

Watts, A. B., Bodine, J. H., Ribe, N. M., 1980. Observations of flexure and the geological evolution of the Pacific Ocean basin. Nature 283 (5747), 532–537, doi: 10.1038/283532a0.

Watts, A. B., ten Brink, U. S., Buhl, P., Brocher, T. M., 1985. A multichannel seismic study of lithospheric flexure across the Hawaiian-Emperor seamount chain. Nature 315 (6015), 105–111, doi: 10.1038/315105a0.

Zamani, A., Samiee, J., Kirby, J. F., 2013. Estimating the mechanical anisotropy of the Iranian lithosphere using the wavelet coherence method. Tectonophysics 601, 139–147. doi: 10.1016/j.tecto.2013.05.005.